Pharmaceutical Biology

http://informahealthcare.com/phb
ISSN 1388-0209 print/ISSN 1744-5116 online
Editor-in-Chief: John M. Pezzuto
Pharm Biol, Early Online: 1–9
 DOI: 10.3109/13880209.2015.1070877

Taylor & Francis
Taylor & Francis Group

ORIGINAL ARTICLE

Anti-endotoxin effects of terpenoids fraction from *Hygrophila auriculata* in lipopolysaccharide-induced septic shock in rats

Md. Sarfaraj Hussain[1,2], Faizul Azam[1], K. F. H. Nazeer Ahamed[2,3], V. Ravichandiran[2], and Ismail Alkskas[1]

[1]*Faculty of Pharmacy, Misurata University, Misurata, Libya,* [2]*Department of Pharmacognosy, Vels College of Pharmacy, Chennai, India, and* [3]*Centre for Research and Innovation (CRI), Faculty of Pharmacy, Asia Metropolitan University, Cheras, Malaysia*

Abstract

Context: *Hygrophila auriculata* (K. Schum) Heine (Acanthaceae) has been traditionally used for the treatment of various ailments such as inflammation, rheumatism, jaundice and malaria.
Objective: The present study aims to separate terpenoid fraction (TF) from alcohol (70%) extract of the whole plant of *Hygrophila auriculata* and assess its anti-inflammatory activity.
Materials and methods: HPTLC analysis of TF was performed for the estimation of lupeol. Edema was induced in Wistar albino rats by subplanter injection of 0.1 ml of 1% (w/v) carrageenan into the right hind paw after 1 h of TF administration (100 and 200 mg/kg oral). Septic shock was induced by intraperitoneal administration of LPS (100 μg/kg) in rats and interleukins (IL-1β and IL-6), tumor necrosis factor (TNF-α), superoxide dismutase (SOD), lipid peroxidation (LPO), and nitric oxide (NO) were measured in serum. AutoDock 4.2 was used for molecular docking.
Results: Administration of TF significantly ($p < 0.005$) restored the serum levels of cytokines, LPO (7.77 ± 0.034 versus 4.59 ± 0.059 nmole of TBARS), NO (9.72 ± 0.18 versus 4.15 ± 0.23 μmol nitrite/mg of wet tissue), and SOD (4.89 ± 0.036 versus 7.83 ± 0.033 Unit/mg protein) compared with the LPS-challenged rats. Analysis of *in silico* results revealed that TNF-α is the most appropriate target in eliciting anti-inflammatory activity.
Conclusion: The present findings suggest that TF of *Hygrophila auriculata* possesses great promise as an anti-inflammatory agent which may be due to its antioxidant effect. Molecular docking results could be exploited for lead optimization and development of suitable treatment of inflammatory disorders.

Keywords

Anti-inflammatory, lupeol, lipid peroxidation, molecular docking, tumor necrosis factor-α

History

Received 12 December 2014
Revised 22 April 2015
Accepted 4 July 2015
Published online 1 October 2015

Introduction

Sepsis and septic shock are still among the most challenging areas of modern medicine. It is a severe form of host systemic inflammatory reaction to infections, which is usually caused by bacterial infections or endotoxin. Endotoxin activates the host effector cells through stimulation of receptors on their surface (Bose et al., 2012). These target cells secrete large quantities of inflammatory cytokines, such as tumor necrosis factor-α (TNF-α), interleukin-1 (IL-1), IL-6, and IL-8, platelet-activating factor (PAF), NO metabolites, erythropoietin, and endothelin (Harizi et al., 2011; Yang et al., 2014). For this reason, new approaches are investigated to treat not only the infection but also to neutralize the biological effect of the endotoxin (Wyska, 2009). Epidemiological studies suggest that consumption of fruits, vegetables, and few herbs is associated with a lower incidence of infection and inflammatory diseases (Guo et al., 2014; Liu et al., 2014). The plant *Hygrophila auriculata* (K. Schum) Heine (Acanthaceae) is a wild herb commonly found in India, Sri Lanka, Burma, Malaysia, and Nepal (Chopra et al., 1986). A survey of ethnobotanical literature found that the roots, seeds, and ashes of the plant have been extensively used in the traditional system of medicine for the treatment of jaundice, hepatic obstruction, rheumatism, inflammation, edema, and gout (Hussain et al., 2009). Based on these observations, the present investigation studied the effect of terpenoids, which are the most abundant phytochemicals of this plant, in lipopolysaccharide (LPS)-induced sepsis in rats.

Molecular docking is a computational method for finding out binding modes of ligands to their targets rapidly and is being applied reliably to drug design and discovery assignments (Azam et al., 2014). It has been shown in the literature that these computational techniques can strongly support and help the design of novel, more potent inhibitors by revealing the mechanism of drug-receptor interactions (Shushni et al., 2013). Therefore, to underscore the possible mode of interaction *in silico*, lupeol was subjected to molecular docking studies utilizing X-ray crystal structures of COX-1, COX-2, and TNF-α.

Correspondence: Dr. Md. Sarfaraj Hussain, Faculty of Pharmacy, Misurata University, Misurata, Libya. Tel: +218 91 6778800. E-mail: dr.mshwinglikeangel@gmail.com

Materials and methods

Plant materials, chemicals, and drugs

The fresh plants of *Hygrophila auriculata* were collected from the field area of Paddapai, Kancheepuram District, Tamil Nadu, India, in January 2007. Samples were authenticated by Dr. P. Jayaraman, Plant Anatomy Research Center, Chennai, India. A voucher Specimen no. PARC 55/01/2007 has been deposited at the herbarium, Department of Pharmacognosy & Phytochemistry, Vel's College of Pharmacy, Pallavaram, Chennai, India. LPS was purchased from Sigma Chemical Co., St. Louis, MO. Indomethacin was procured from Ranbaxy Labs, New Delhi. Other chemicals, solvents and kits are purchased from SISCO Research Lab, Mumbai, India.

Extraction

The dried and powdered aerial parts of *H. auriculata* (7 kg) were macerated with 95% w/v ethanol. The ethanol extract was with *n*-butanol in Soxhlet because it is a widely used modest polar solvent for the solubilization of various terpenoids (Cheng et al., 2014). The *n*-butanol soluble portion was concentrated to dryness and 150 g residue was obtained. The residue has shown only positive tests (qualitative) for terpenoids (Nollers reagent) and hence it was labeled as terpenoid fraction (TF). TF was purified by silica gel column chromatography using ethyl acetate.

Quantitative estimation of lupeol using high-performance thin-layer chromatography (HPTLC) fingerprinting

Chromatography was performed, as described previously (Hussain et al., 2012a,b) on 20 cm × 10 cm aluminum Lichrosphere HPTLC plates precoated with 200 μm layers of silica gel $60F_{254}$ (E. Merck, Darmstadt, Germany). The TF (dissolved in pure methanol 10 μl) was spotted in the form of a band using a CAMAG Linomat-V automatic applicator equipped with a 100 μl syringe (CAMAG, Muttenz, Switzerland) (Figure 1). The constant application rate was 160 nl s^{-1}. Linear ascending development with toluene:methanol:formic acid (7.0:2.7:0.3, v/v/v) as the mobile phase was performed in a 20 cm × 10 cm twin-trough glass chamber (CAMAG, Muttenz, Switzerland), previously saturated with the mobile phase for 15 min at room temperature (25 ± 2 °C) and relative humidity 60 ± 5%. The development distance was 8 cm (development time 10 min) and 20 ml mobile phase was used. The plates were dried at room temperature in air and warmed (at 75 °C for 5 min) to identify compact bands. Densitometric analysis was performed at 530 nm in reflectance mode with a Camag TLC scanner III (CAMAG, Muttenz, Switzerland) operated by WinCATS software (Version 1.2.0) (CAMAG, Muttenz, Switzerland). The slit dimensions were 5 mm × 0.45 mm and the scanning speed of 20 mm s^{-1}.

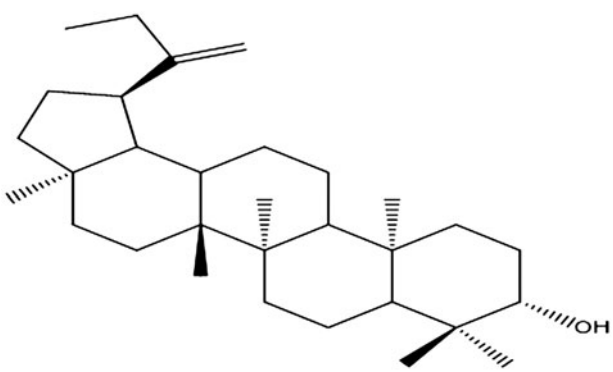

Figure 1. Chemical structure of lupeol.

Animals

Wistar albino rats (200 ± 50 g) and Swiss albino mice (25–30 g) of both sexes were used in this investigation. The animals were kept in the propylene cages and maintained at a temperature of 25 ± 2 °C and had access to food and water *ad libitum*. The study was approved by institutional animal ethics committee (IAEC) of CPCSEA (Approval No: CPCSEA/12-12-00/PH-07-04).

Preliminary acute toxicity studies

Mice were divided into two groups of six each. Vehicle control group received 0.2% CMC and second group was treated with starting dose of 2000 mg/kg orally and the maximum dose of 5000 mg/kg of TF suspended in 0.2% CMC. Immediately after the dose, animals were observed continuously for first 4 h and next 14 d to record mortality.

Carrageenan-induced paw edema in rats

Edema was induced by subplanter injection of 0.1 ml of 1% freshly prepared suspension of carrageenan into the right hind paws of the rats. The first group of animals which served as control was treated with 0.3% CMC. The second group of animals was treated with carrageenan (1%). The third group of animals was treated with standard drug, indomethacin (5 mg/kg). Fourth and fifth groups of animals were treated with TF at two different doses (100 and 200 mg/kg). The volume of the injected paws and contra-lateral paws were measured at 1, 2, 3, 4, and 5 h intervals using Plethysmometer (Mukherjee et al., 1997).

Animal grouping and LPS treatment

Septic shock was induced by intraperitoneal (i.p.) injection of 100 μg of LPS from *Escherichia coli* 055:B5 (Sigma-Aldrich, St. Louis, MO) in sterile pyrogen free 0.9% saline. After i.p administration of LPS, animals were monitored for body temperature, heart rate, and any neurotoxic behavior. Thirty rats were randomly divided into five groups (six rats per group) as follows:

Group I: control rats received vehicle sterile pyrogen free 0.9% saline.

Group II: LPS control rats received vehicle sterile pyrogen free 0.9% saline.

Group III: LPS rats treated with indomethacin (5 mg/kg body wt.) after 1 h LPS treatment.

Group IV: LPS rats treated TF 100 mg/kg, body wt. after 1 h LPS treatment.

Group V: LPS rats treated with TF 200 mg/kg, body wt. after 1 h LPS treatment

Animals were exsanguinated at 24 h after LPS treatment; blood was collected and divided into two portions. One portion of the blood was used to quantify hematocrit, total WBC, platelet count and neutrophil count, and other portion was allowed to clot at room temperature for 15–20 min and centrifuged at 4 °C for 20 min ($1500 \times g$) and the serum was separated for the estimation cytokines, TNF-α and nitrates level. Liver tissue was collected and weighed. Approximately 100–150 mg of tissue samples were homogenized with ice cold phosphate buffer saline (PBS) containing cocktail protease inhibitor at 4 °C for 20 min ($1500 \times g$) and supernatants were aliquot into smaller volumes, stored at −20 °C until the antioxidant assays.

Measurement of cytokines and TNF-α

Serum concentrations of IL-1β, IL-6, and TNF-α were measured by ELISA using commercially available kit (Endogen, Woburn, MA).

Hematological analysis

The hematological parameters like hemoglobin (Hb), RBC, WBC and platelets were determined by the usual standardized laboratory method (Dacie & Lewis, 1977).

Measurement of superoxide dismutase (SOD) in liver homogenate

SOD activity in liver tissue was measured by reported method (Beauchamp & Fridovich, 1971). SOD measurement was carried out by the ability of SOD to inhibit spontaneous oxidation of adrenaline to adrenochrome. A mixture of 2.80 ml of sodium carbonate (0.05 mM) buffer (pH 10.2), 100 µl of EDTA (1.0 mM) and 20 µl of liver homogenate or sucrose (blank) will be incubated at 30 °C for 45 min. Thereafter, the reaction was imitated by adding 100 µl of adrenaline solution (9.0 mM). The change in the absorbance was recorded at 480 nm for 8–12 min. Similarly, SOD calibration curve was prepared by taking 10 units/ml a standard solution. One unit of SOD produced approximately 50% inhibition of auto-oxidation of adrenaline. The results are expressed as SOD µmoles/mg tissue.

Measurement of lipid peroxidation (LPO) in liver homogenate

Estimation of LPO in liver tissue was carried out by measuring the LPO end product malondialdehyde (MDA) by the method of Okhawa et al. (1979). Liver homogenate (0.1 ml) was treated with 20% of 1.5 ml of acetic acid (pH 3.5), 1.5 ml thio barbituric acid, and 0.2 ml sodium dodecyl sulfate (8.1%). The mixture was then heated at 100 °C for 60 min. The mixture was cooled with tap water and 5 ml of *n*-butanol-pyridine (15:1% v/v), 1 ml of distilled water was added. The mixture was shaken vigorously. After centrifugation at 4000 rpm for 10 min, the organic layer was withdrawn and the absorbance was measured at 532 nm. The concentration of MDA formed is expressed as nM/mg of protein.

Measurement of NO: Griess reaction

After the experiment, animals were sacrificed and the liver tissues were washed with PBS (pH 7.4) and placed on ice as method described earlier (Sajjad et al., 2009). Briefly, a 50 µl sample was added with 100 µl of Griess reagent and the reaction mixture was incubated for about 5–10 min at room temperature, protected from light. The optical density was measured at 540 nm in microplate reader according to the protocol of the reagent manufacturer. Calculations were done after generating a standard curve from sodium nitrite in the same buffer as used for preparation of homogenate.

Molecular-docking studies

Three-dimensional coordinates of COX-1, COX-2, and TNF-α were obtained from the Protein Data Bank. Discovery Studio Visualizer and AutoDock Tools packages were used to prepare docking files. For each PDB structural data file containing protein and ligand complex, the ligand was extracted from protein complex in PDB file. The partial atomic charges were calculated with the aid of Gasteiger method and after merging non-polar hydrogens, rotatable bonds were assigned. All the amide bonds were considered as non-rotatable. For the protein, the hetero-atoms including cofactors, water molecules and the ligands were removed.

Structure of lupeol was drawn in ChemBioDraw Ultra 12.0 (ChemBioOffice, New Jersey, CA) and converted to its three-dimensional structure in ChemBio3D Ultra 12.0 (ChemBioOffice, New Jersey, CA), energy minimized by the PM3 method using MOPAC Ultra 2009 program (ChemBioOffice, New Jersey, CA), (http://OpenMOPAC.net) and saved as in pdb format. The prepared ligand was used as an input file for AutoDock 4.2 in the next step. Lamarckian genetic algorithm method was employed for docking simulations (Morris et al., 1998). The standard docking procedure was used for a rigid protein and a flexible ligand whose torsion angles were identified (for 10 independent runs per ligand). A grid of 60, 60, and 60 points in *x*, *y*, and *z* directions was built with a grid spacing of 0.375 Å and a distance-dependent function of the dielectric constant were used for the calculation of the energetic map. The default settings were used for all other parameters. At the end of docking, the best poses were analyzed for hydrogen bond interactions and root mean square deviation (RMSD) calculations using Discovery Studio Visualizer 2.5 program (Accelrys Inc., San Diego, CA). From the estimated free energy of ligand binding ($\Delta G_{binding}$, kcal/mol), the inhibition constant (K_i) for the ligand was calculated (Table 5).

Statistical analysis

Data in each group are expressed in mean ± SD. Data were analyzed by one-way ANOVA followed by the Tukeys multiple comparison test using Graphpad PRISM 5 Software (GraphPad Inc., La Jolla, CA). Probability $p < 0.05$ is considered as significant.

Results and discussion

Since ancient times, natural products have been used as remedies to treat human diseases. *Hygrophila auriculata* has

been advocated for the treatment of variety of diseases including inflammation and diabetes. In traditional medicine practice the roots, seeds, and aerial parts of the plant have been used for the treatment of jaundice, hepatic obstruction, rheumatism, inflammation, urinary infection, gout, malaria and impotence, increasing its potential for being developed into a modern herbal product (Hussain et al., 2012a,b). Lupeol, a phytosterol and triterpene, is often found in edible fruits and vegetables. Lupeol is reported to exhibit a spectrum of pharmacological activities against various disease conditions. These include conditions such as inflammation, arthritis, diabetes, cardiovascular ailments, renal disorder, hepatic toxicity, microbial infections, and cancer (Hussain et al., 2012a,b; Siddique & Saleem, 2011; Sudhahar et al., 2008a,b). The available literature suggests that lupeol is a non-toxic agent and does not cause any systemic toxicity in animals at doses ranging from 30 to 2000 mg/kg (Murtaza et al., 2009). Lupeol has been shown to target molecules which are known to play a key role in the development of various human ailments. It is noteworthy that lupeol has been reported to selectively target diseased and unhealthy human cells, while sparing normal and healthy cells. Published studies provide evidence that lupeol modulates the expression or activity of several molecules such as cytokines IL-2, IL4, IL5, ILβ, proteases, α-glucosidase, cFLIP, Bcl-2, and NFκB (Yang et al., 2014).

Chromatography

Chromatogram were developed for lupeol under chamber saturation conditions using toluene–methanol–formic acid (7.0:2.7:0.3, v/v/v) as the mobile phase or the solvent system (Figure 2). The same mobile phase has been also employed for the separation of TF of *H. auriculata* (Figure 2). The optimized saturation time was found to be 10 min. UV spectra measured for the spots showed maximum absorbance at about 530 nm; therefore, UV densitometric analysis was performed at 530 nm in the reflectance mode as HPTLC-UV 530 nm (CAMAG, Muttenz, Switzerland). Compact bands as sharp, symmetrical, and with high resolution were obtained at R_f 0.52 ± 0.02 for lupeol (Figure 3). Lupeol were well resolved at R_f 0.52 from TF of *H. auriculata* sample in the solvent system as same used in case of standards (Table 1). The plates were visualized at different wavelengths 254, 366, and 530 nm as the compounds were found to absorb at variable spectrum range (Figures 2 and 3). The identity of the bands of compounds **1**–**7** in the sample extracts was confirmed by overlaying their UV absorption spectra with those of the standards at 530 nm (Table 2).

Preliminary acute toxicity studies

From acute toxicity studies, it was observed that the administration of butanol fraction (TF) of *H. auriculata* to mice did not induce drug-related toxicity and mortality in the animals. The treated animals were well tolerated and exhibited normal behavior up to 5 g/kg body wt. orally. All animals were alert with normal grooming, touch response, pain response; and there was no sign of passivity, stereotypy, and vocalization. Their motor activity and secretary signs were also normal.

Carrageenan-induced rat paw edema

The effect of indomethacin and terpenoid fraction from *H. auriculata* on carrageenan induced rat paw is shown in Figure 4. Administrations of carrageenan to normal animals showed significant ($p < 0.05$) increase in paw inflammation from 1 h to 5 h when compared with control. Paw edema in rats reached its peak at 4 h after carrageenan administration. Per oral treatment of indomethacin showed significant reduction paw volume in rats from 2 h Interestingly

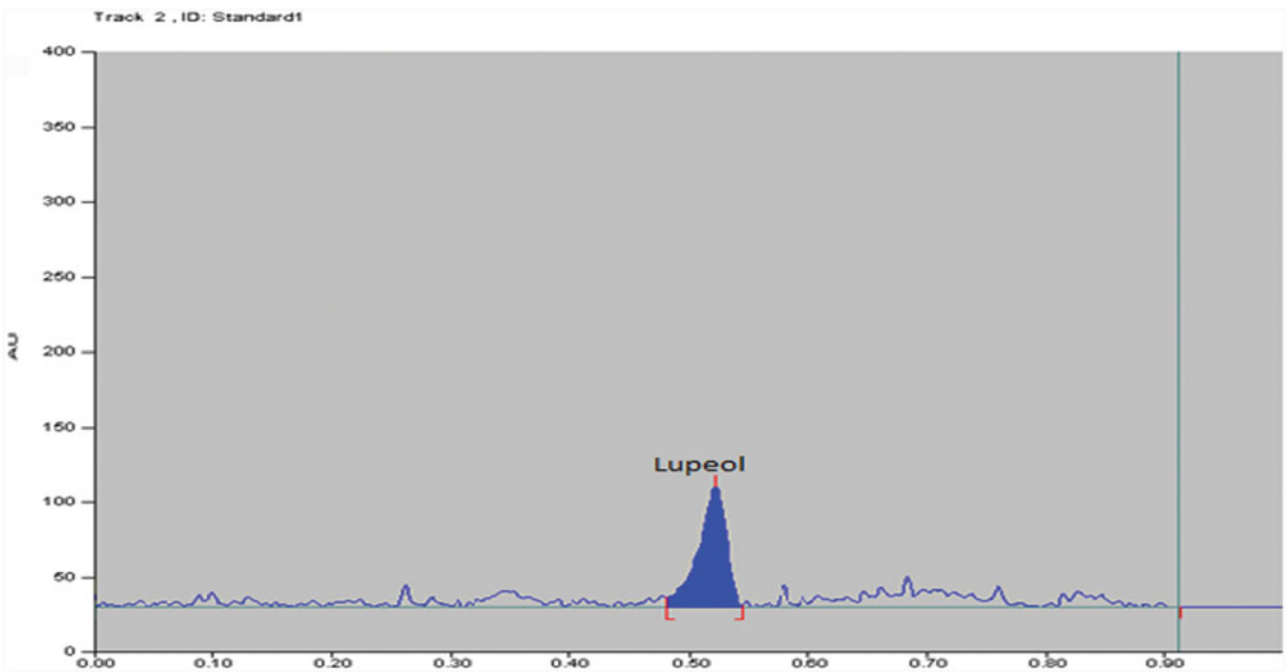

Figure 2. HPTLC chromatogram of the standard lupeol structure at RF 0.52.

administration various dose of TF (100 and 200 mg/kg) produced a significant inhibition ($p < 0.05$) of paw volume in rats treated with carrageenan administration. However, the effect of TF (100 mg/kg) was higher in reducing inflamed paw volume than higher dose.

LPS-induced systemic inflammation in rats – effect of indomethacin and TF on TNF-α, IL-1β, and IL-6

Effect of indomethacin and terpenoid fraction from *H. auriculata* on LPS-induced TNF-α, IL-1β and IL-6 expression in serum is shown in Figure 5(A)–(C). Animals treated with LPS showed over expression of TNF-α in serum after 24 h. The expression was significant ($p < 0.05$) when compared with control animals. Pre-treatment of TF and indomethacin showed decrease in the expression of TNF-α, IL-1β, and IL-6 in serum of the rats treated with LPS. The standard drug indomethacin showed significant effect ($p < 0.05$) in decreasing TNF-α, IL-1β, and IL-6 than TF.

Hematological parameters

After administration of LPS, there was significant decrease in RBC count, hemoglobin from normal levels, and significant increase in total WBC count and platelets levels above the normal. However, as shown in Table 3, the administration of TF and indomethacin is shown significant to increase the hemoglobin and RBC content when compared with the control group. However, TF- and indomethacin-treated groups significantly decreased the total WBC count and platelets.

Effects of terpenoids fraction of *H. auriculata* treatment restored SOD levels

The concentration of SOD activity was measured to estimate endogenous defenses against superoxide anions. A marked decrease in SOD ($p < 0.05$) concentrations were found in the liver of LPS rats. Treatment with TF and indomethacin significantly inhibited reduction in SOD level as compared with the LPS group (Table 4).

Effects of terpenoids fraction of *H. auriculata* treatment decreased TBARS

The effect of TF of *H. auriculata* on TBARS level was studied to understand the role of oxidative stress. A significant increase ($p < 0.05$) in TBARS level was observed in the LPS group as compared with the control group. Treatment with TF

Table 1. R_F, linear regression data for the calibration curve and sensitivity parameter for lupeol.

Parameter	Lupeol
R_F	0.52
Linearity range (ng band^{-1})	100–1000
Regression equation	$Y = 0.0059X + 0$
Correlation coefficient (r^2)	0.9994
Slope ± sd	0.0059 ± 0.0008
Intercept ± sd	Nil
Standard error of slope	0.0011
Standard error of intercept	na[a]
LOD	45
LOQ	135

[a]Not available.

Table 2. Lupeol contents estimated in terpenoid fraction of *Hygrophila auriculata* by developed method.

	Lupeol[a]	
	Content (ng spot^{-1})	%RSD
Terpenoid fraction of *Hgrophila auriculat*a	79.0	1.58

[a]Volume applied in each replicate was ten microlitres.

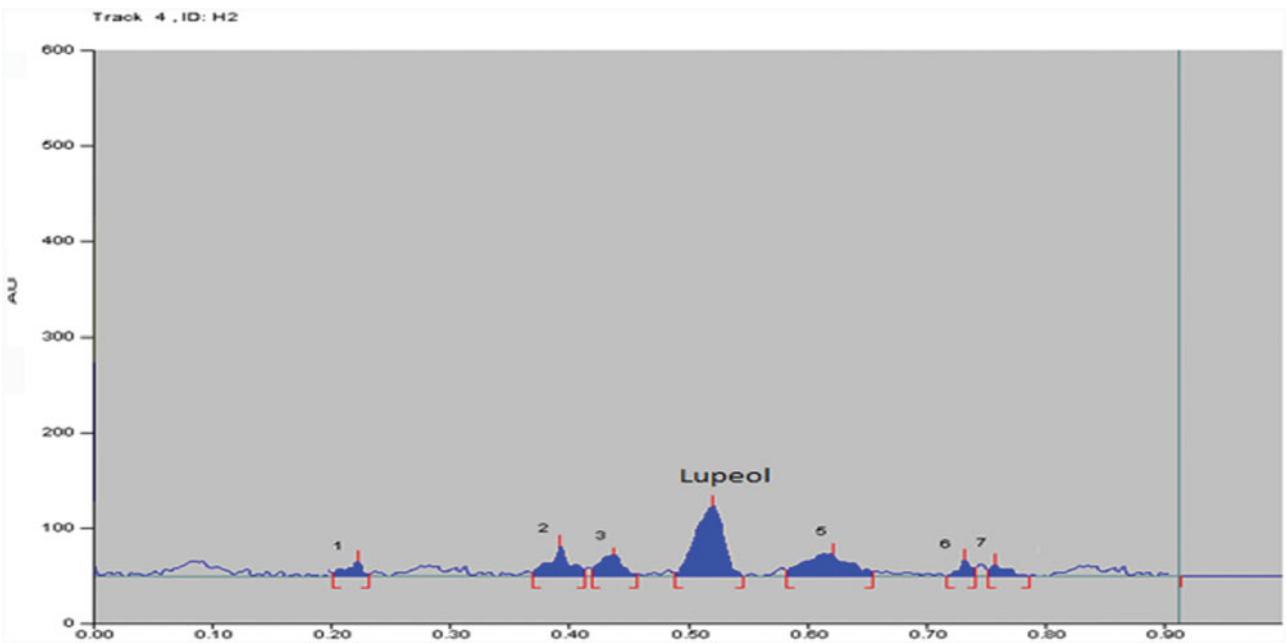

Figure 3. HPTLC chromatogram of terpenoid fraction of *H. auriculata* scanned at 530 nm [peaks 1–7; lupeol (0.52)].

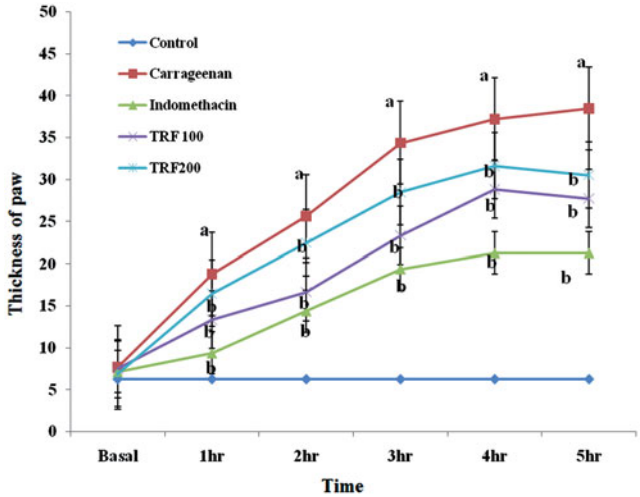

Figure 4. Effect of indomethacin and terpenoid fraction of *H. auriculata* on carrageenan-induced rat paw inflammation.

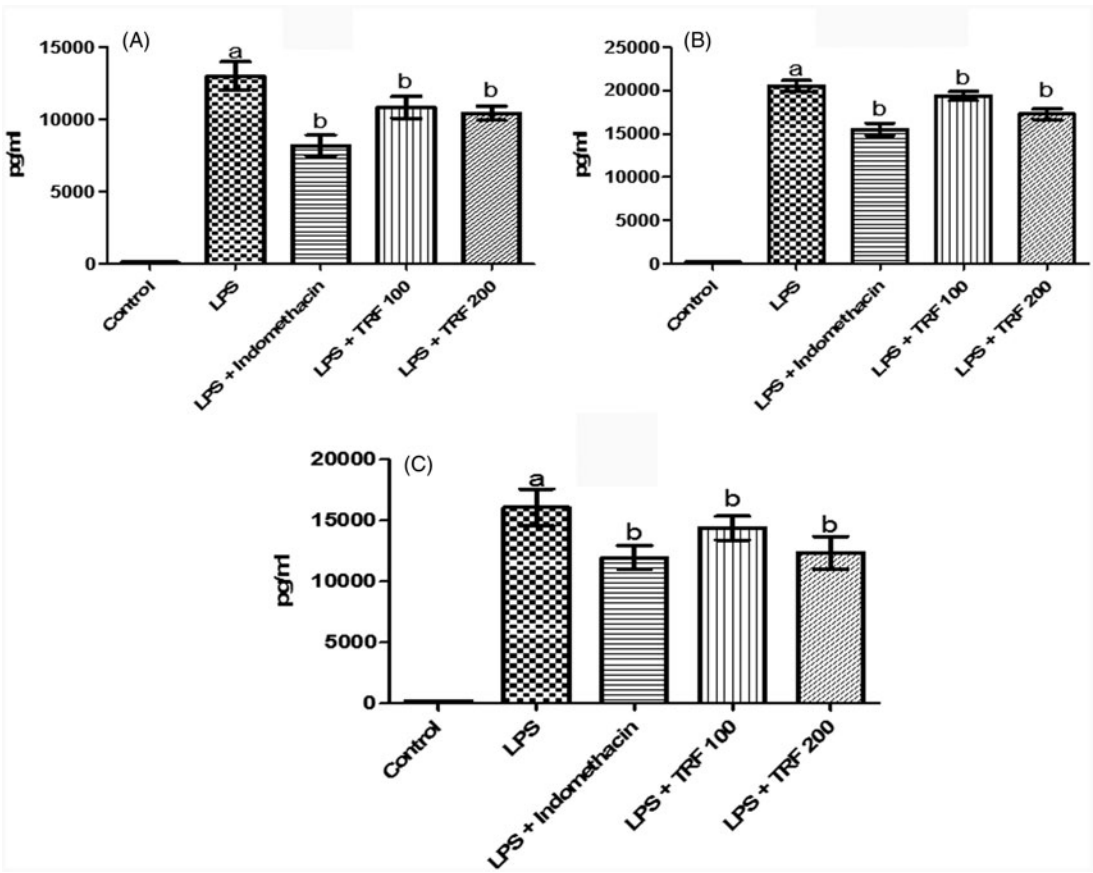

Figure 5. Effect of indomethacin and terpenoid fraction on LPS-induced cytokine (A) TNF-α, (B) IL 1β, and (C) IL 6 in rat plasma.

of *H. auriculata* and indomethacin decreased TBARS level by inhibiting lipid peroxidation in the liver tissue (Table 4).

Effects of terpenoids fraction of *H. auriculata* treatment on nitric oxide

A significant increase in nitrite was observed in the LPS group as compared with control. The treatment with TF of *H. auriculata* and indomethacin declined the increase in the nitrite levels significantly as compared with the LPS group (Table 4).

Molecular docking

Validation of docking protocol

A prerequisite to any successful experiment is the validation step. The docking protocol used in the present study was, therefore, validated by docking all native co-crystallized ligand molecules to their respective proteins. According to the method of validation, if the RMSD of the best docked conformation is $\leq$2.0 Å from the experimental one, the used scoring function is successful (Azam et al., 2012a,b).

Table 3. Effect of terpenoid fraction of *Hygrophila auriculata* in hematological parameters in control and experimental animals.

Groups	Control	AIA	LPS + IDM (10 mg)	LPS + TF (100 mg)	LPS + TF (200 mg)
RBC (millions/mm^3)	8.98 ± 0.26	7.16 ± 0.18^a	8.98 ± 0.29^b	8.72 ± 0.21^b	9.02 ± 0.14^b
WBC (thousands/mm^3)	7.95 ± 0.65	12.96 ± 0.68^a	7.96 ± 0.34^b	8.59 ± 0.56^b	7.88 ± 0.83^b
Hb (g/dl)	14.76 ± 1.38	9.89 ± 1.96^a	13.79 ± 1.18^b	13.92 ± 1.92^b	14.78 ± 1.30^b
Platlets (lakhs/ml)	2.46 ± 0.32	3.67 ± 0.85^a	2.61 ± 0.79^b	2.29 ± 0.14^b	2.53 ± 0.28^b

Data are expressed as mean ± SEM of ($n = 6$) rats. Probability $p < 0.05$ is considered as significant.
[a]$p < 0.05$, control versus the induced group.
[b]$p < 0.05$, treatment versus the induced group.

Table 4. Effect of terpenoid fraction of *Hygrophila auriculata* treatment on SOD activity, lipid peroxidase, and nitrite in liver of rats.

Groups	Control	LPS	LPS + IDM (10 mg)	LPS + TF (100 mg)	LPS + TF (200 mg)
SOD (unit/mg protein)	9.42 ± 0.061	4.89 ± 0.036^a	6.58 ± 0.35^b	6.15 ± 0.032^b	7.83 ± 0.033^b
LPO (nmole of TBARS formed/h/mg protein)	2.44 ± 0.056	7.77 ± 0.034^a	5.6 ± 0.10^b	5.48 ± 0.045^b	4.59 ± 0.059^b
Nitric oxide (μmol nitrite/mg of wet tissue)	3.06 ± 0.010	9.72 ± 0.18^a	4.78 ± 0.28^b	5.39 ± 0.042^b	4.15 ± 0.23^b

Data are expressed as mean ± SEM of ($n = 6$) rats. Probability $p < 0.05$ is considered as significant.
[a]$p < 0.05$, control versus the induced group.
[b]$p < 0.05$, treatment versus the induced group.

Table 5. Docking results of lupeol with COX-1, COX-2 and TNF-α.

				Hydrophobic interactions			H-bond interactions		
Target	ΔG_b[a]	K_i[b]	RMSD[c] (Å)	Type	Amino acids	Dist[d] (Å)	Comp	Amino acids	Dist[d] (Å)
1EQG	−2.74	9.87 mM	10.07	–	–	–	O	Phe-470	2.97
1CX2	−4.06	1.06 mM	3.37	π-σ	Phe-518	3.82	–	–	–
				π-Alkyl	Tyr-355	4.68			
				π-Alkyl	Tyr-355	3.93			
				π-Alkyl	Trp-387	4.25			
				π-Alkyl	Phe-518	4.52			
2AZ5	−6.84	9.68 μM	5.01	π-Alkyl	Tyr-59	5.17	–	–	–
				π-Alkyl	Tyr-59	4.89			
				π-Alkyl	Tyr-59	5.39			
				π-Alkyl	Tyr-119	5.32			
				π-Alkyl	Tyr-119	5.46			
				π-Alkyl	Tyr-151	4.19			
				π-Alkyl	Tyr-151	5.28			
				π-Alkyl	Tyr-151	5.31			
				π-Alkyl	Tyr-151	4.88			

[a]Binding free energy (kcal/mol).
[b]Inhibition constant estimated by docking.
[c]Root mean square deviation (in Å).
[d]Bond distance (in Å).

The RMSD values of the native co-crystallized ligands after docking were ≤2.0 Å (data not shown), which confirms the reliability of AutoDock for docking of lupeol into crystal structures of different anti-inflammatory drug targets.

Binding interactions of lupeol with anti-inflammatory drug targets

Molecular docking is a computational method to find out binding modes of ligands to their receptors rapidly, and is being relied in drug design and discovery programs. The intent of this technique is to swap experimental studies of protein–ligand complexes by modeling their structures and binding affinities *in silico*. It is regularly used to predict the binding positioning of drug candidates to their protein targets in order to predict the affinity and activity of the test molecules. With an instrument that can correctly and consistently predict protein–ligand structure, one could easily identify the right molecules to modulate functions of the desired protein, for example, a therapeutic target. To predict the mode of binding interaction of lupeol at the receptor site that may be responsible for governing the observed anti-inflammatory activity, it was docked into the X-ray crystal structures of three different targets using AutoDock 4.2 program (Morris et al., 1998). For each docking experiment, the lowest energy docked structure was selected from 10 runs. The binding affinity was evaluated in terms of binding free energies (ΔG_b, kcal/mol), inhibition constants (K_i), hydrogen bonding, π–π interactions, and RMSD values (Table 5).

Results of the molecular docking study revealed that the lupeol docked into the active sites of cyclooxygenase-1, cyclooxygenase-2, and tumor necrosis factor-alpha (PDB

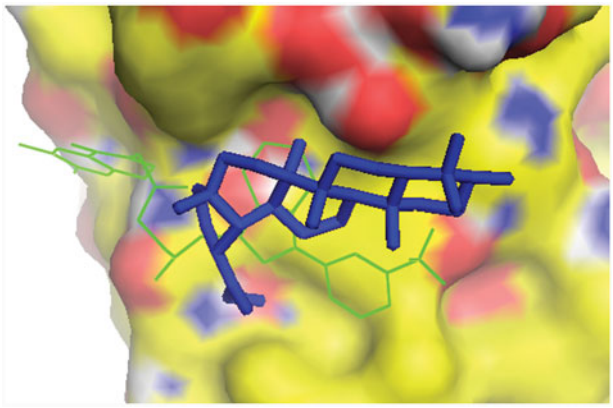

Figure 6. The lowest energy configuration of docking result of lupeol (shown as stick in blue color) with binding pocket of TNF-α. The residues of binding pocket are shown as surface. Native co-crystallized ligand, an inhibitor of TNF-α is shown as line in green color.

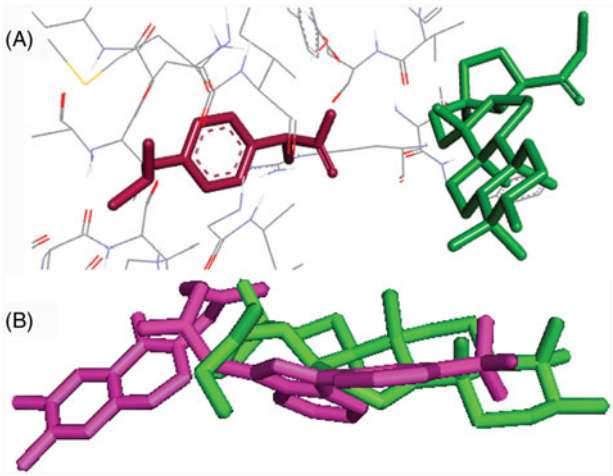

Figure 7. Docking conformation of lupeol (green, right hand side) in COX-1 failed to occupy the area of binding pocket engaged by the native inhibitor (dark pink, left hand side) exhibiting RMSD of 10.13 A (A); the docked lupeol (green, right hand side) occupying the same position as native TNF-α inhibitor (magenta, left hand side) demonstrating RMSD of 5.01 A (B).

code: 1EQG, 1CX2, and 2AZ5, respectively) exhibited their binding interactions in a similar fashion to the native co-crystallized ligands of the respective enzymes (Table 5).

Analysis of the docking results revealed that lupeol accommodates most comfortably in the binding pocket of TNF-α (Figures 6 and 7), exhibiting a binding energy of −6.84 kcal/mol, while higher binding energies were noted in case of other macromolecular targets. Similarly, calculated inhibition constant was least in case of TNF-α suggesting that this enzyme is the most favorable target for lupeol.

Investigations of the docked conformations of TNF-α and lupeol revealed that carbon skeleton provides sites for receptor interaction by hydrophobic interaction in the binding pocket (Figure 6). With these findings, we hope that the results will facilitate the understanding of mode of interaction of lupeol with various macromolecular targets that will be vital in lead modification and design of potent anti-inflammatory drugs.

Conclusion

In our present study, the TF fraction separated from *H. auricualta* extract demonstrated anti-inflammatory activity at two different dose levels in carrageenan induced rat paw edema as well as LPS-induced systemic inflammation in rats. In carrageenan-induced rat paw edema model, the anti-inflammatory effect of standard drug indomethacin and TF at two different doses was observed from 60 min after carrageenan challenge. Administration of TF 100 mg/kg body weight showed decrease in paw edema volume from 1 h to 4 h and it sustains its anti-inflammatory effect after 4 h. Interestingly both dose levels of TF fraction exhibited similar pattern in reducing carrageenan-induced paw edema from 1 h to till the end of the experiment. However, the anti-inflammatory response observed in 100 mg/kg was higher than the 200 mg/kg body wt. LPS-induced systemic inflammation model clearly reveals the beneficial effect of indomethacin and TF (100 & 200 mg/kg body wt) in inhibiting over expressed pro-inflammatory mediators namely TNF-α, IL-1β, and IL-6 in rat serum treated with LPS. Ingestion of TF (100 and 200 mg/kg body wt.) exhibited their anti-inflammatory effect by reducing the levels of pro-inflammatory markers in the serum of LPS-treated rats. With these findings, we hope that the results will facilitate the understanding of mode of interaction of lupeol with various macromolecular targets that will be vital in lead modification and design of potent anti-inflammatory drugs.

Acknowledgements

The authors are thankful to the Prof. (Dr.) P. Jayaraman, Plant Anatomy Research Centre, Chennai, Tamil Nadu, for providing authenticated sample of *Hygrophila auriculata*.

Declaration of interest

The authors declare no conflict of interest.

References

Azam F, Amer AM, Abulifa AR, Elzwawi MM. (2014). Ginger components as new leads for the design and development of novel multi-targeted anti-Alzheimer's drugs: A computational investigation. *Drug Des Devel Ther* 8:2045–59.

Azam F, Prasad MVV, Thangavel N. (2012a). Structure-based design, synthesis and molecular modeling studies of 1-(benzo[*d*]thiazol-2-yl)-3-(substituted aryl) urea derivatives as novel anti-Parkinsonian agents. *Med Chem Res* 21:2630–43.

Azam F, Prasad MV, Thangavel N, et al. (2012b). Structure-based design, synthesis and molecular modeling studies of thiazolyl urea derivatives as novel anti-Parkinsonian agents. *Med Chem* 8:1057–68.

Beauchamp C, Fridovich I. (1971). Superoxide dismutase: Improved assays and an assay applicable to acrylamide gels. *Anal Biochem* 44: 276–87.

Bose S, Song MY, Nam JK, et al. (2012). *In vitro* and *in vivo* protective effects of fermented preparations of dietary herbs against lipopolysaccharide insult. *Food Chem* 134:758–65.

Cheng D, Zhang Y, Gao D, Zhang H. (2014). Antibacterial and anti-inflammatory activities of extract and fractions from *Pyrrosia petiolosa* (Christ et Bar.) Ching. *J Ethnopharmacol* 155:1300–5.

Chopra RN, Nayer SL, Chopra IC. (1986). *Glossary of Indian Medicinal Plants*. New Delhi, India: National Institute of Science and Communication. C.S.I.R Publication.

Dacie, JV, Lewis SM. (1977). *Practical Hematology*, vol. 5. Edinburgh: Churchill Livingstone, 79–160.

Guo Y, Sakulnarmrata K, Konczak I. (2014). Anti-inflammatory potential of native Australian herbs polyphenols. *Toxicol Rep* 1: 385–90.

Harizi H, Chaabane F, Ghedira K, Chekir-Ghedira L. (2011). Inhibition of proinflammatory macrophage responses and lymphocyte proliferation *in vitro* by ethyl acetate leaf extract from *Daphne gnidium*. *Cell Immunol* 267:94–101.

Hussain MS, Fareed S, Ali M. (2012a). Hyphenated chromatographic analysis of bioactive gallic acid and quercetin in *Hygrophila auriculata* (K. Schum) Heine growing wildly in marshy places in India by validated HPTLC method. *Asian Pac J Trop Biomed* 5: S477–83.

Hussain MS, Fareed S, Ali M. (2012b). Simultaneous HPTLC-UV530 nm analysis and validation of bioactive lupeol and stigmasterol in *Hygrophila auriculata* (K. Schum) Heine. *Asian Pac J Trop Biomed* 5:S612–17.

Hussain MS, Nazeer Ahamed KFH, Ravichandiran V, Ansari MZH. (2009). Free radical scavenging capacity of natural terpenes from *Hygrophila auriculata* (Schum) Heine. *Asian J Trad Med* 4:179–87.

Liu L, Hua Y, Wang D, et al. (2014). A sesquiterpene lactone from a medicinal herb inhibits proinflammatory activity of TNF-α by inhibiting ubiquitin-conjugating enzyme UbcH5. *Chem Biol* 21: 1341–50.

Morris GM, Goodsell DS, Halliday RS, et al. (1998). Automated docking using a Lamarckian genetic algorithm and an empirical binding free energy function. *J Comp Chem* 19:1639–62.

Mukherjee PK, Saha K, Das J, et al. (1997). Studies on the anti-inflammatory activity of rhizomes of *Nelumbo nucifera*. *Planta Med* 63:367–9.

Murtaza I, Saleem M, Adhami VM, et al. (2009). Suppression of cFLIP by lupeol, a dietary triterpene, is sufficient to overcome resistance to TRAIL-mediated apoptosis in chemo resistant human pancreatic cancer cells. *Cancer Res* 69:1156–65.

Okhawa H, Ohishi N, Yagi K. (1979). Assay for lipid peroxides in animal tissues by thiobarbituric acid reaction. *Ann Biochem* 95: 351–8.

Sajjad M, Zargan J, Chawla R, et al. (2009). Hippocampal neurodegeneration in experimental autoimmune encephalomyelitis (EAE): Potential role of inflammation activated myeloperoxidase. *Mol Cell Biochem* 328:183–8.

Shushni MA, Azam F, Lindequist U. (2013). Oxasetin from *Lophiostoma* sp. of the Baltic Sea: Identification, *in silico* binding mode prediction and antibacterial evaluation against fish pathogenic bacteria. *Nat Prod Commun* 8:1223–6.

Siddique HR, Saleem M. (2011). Beneficial health effects of lupeol triterpene: A review of preclinical studies. *Life Sci* 88:285–93.

Sudhahar V, Ashok Kumar S, Varalakshmi P, Sujatha V. (2008a). Protective effect of lupeol and lupeol linoleate in hypercholesterolemia associated renal damage. *Mol Cell Biochem* 317:11–20.

Sudhahar V, Veena CK, Varalakshmi P. (2008b). Antiurolithic effect of lupeol and lupeol linoleate in experimental hyperoxaluria. *J Nat Prod* 71:1509–12.

Wyska E. (2009). Pretreatment with R (+)-verapamil significantly reduces mortality and cytokine expression in murine model of septic shock. *Int Immunopharmacol* 9:478–90.

Yang M, Lin HB, Gong S, et al. (2014). Effect of *Astragalus* polysaccharides on expression of TNF-α, IL-1β and NFATc4 in a rat model of experimental colitis. *Cytokine* 70:81–6.